

CONJUGATE SYMMETRIC SEQUENCY ORDERED WALSH FOURIER TRANSFORM

Soo-Chang Pei, Chia-Chang Wen

Department of Electrical Engineering, National Taiwan University, Taipei, Taiwan, R.O.C
Email address: pei@cc.ee.ntu.edu.tw

ABSTRACT

A new family of transforms, which is called the conjugate symmetric sequency-ordered generalized Walsh-Fourier transform (CS-SGWFT), is proposed in this paper. The CS-SGWFT generalized the existing transforms including the conjugate symmetric sequency ordered complex Hadamard transform (CS-SCHT) and the discrete Fourier transform (DFT) as the special cases of the CS-SGWFT. Like the CS-SCHT and the DFT, the spectrums of the CS-SGWFT for real input signals are conjugate symmetric so that we need only half memory to store the transform results. The properties of the CS-SGWFT are similar to those of the CS-SCHT and DFT, including orthogonality, sequency ordering, and conjugate symmetric. Meanwhile, the proposed CS-SGWFT has radix-2 fast algorithm. Finally, applications of the CS-SGWFT for image noise removal and spectrum estimation are proposed.

Index Terms—Hadamard transform, Walsh transform, Discrete Fourier transform, Sequency ordered, Conjugate symmetric

1. INTRODUCTION

The discrete orthogonal transform (DOT) is widely used many applications. Recent researches are focus on the generalization to Walsh Hadamard transform (WHT), including unified complex Hadamard transform (UCHT) [1], sequency ordered complex Hadamard transform (SCHT) [2], conjugate symmetric sequency orderd complex Hadamard transform (CS-SCHT) [3], sequency ordered generalized Walsh Fourier transform (SGWFT) [4], are proposed.

In [3], the rows of conjugate symmetric sequency orderd complex Hadamard transform (CS-SCHT) matrix are arranged in ascending order so that it has sequency ordered property. Moreover, the CS-SCHT spectrum is conjugate symmetry for real input signals which reveals that we can save half memory size to store the transform values. The CS-SCHT also has $M\log_2 N$ fast algorithms.

In [4], the SGWFT tune the transform behavior among the WHT, SCHT and the DFT by a single parameter p . It is shown that the properties of the SGWFT include unitary, reciprocal inverse, conditional shift invariant, radix 2 fast algorithms. Despite the flexibility and well structured of the SGWFT, it lacks of the conjugate symmetric property like the CS-SCHT so that for real input the SGWFT need as double memory size to store the transform value as the CS-SCHT does. In [5], the conjugate symmetric discrete orthogonal transform (CS-DOT) provide a systematic way to generate the orthogonal matrix with conjugate symmetric property which generalize the CS-SCHT and DFT.

In this paper, we propose the conjugate symmetric sequency ordered generalized Walsh Fourier transform (CS-SGWFT) as special cases of the CS-DOT. The CS-SGWFT not only has the properties and the flexibility like the SGWFT but it also fits the conjugate symmetric property like the CS-SCHT. We will use the CS-DOT generating method with specific generating function to generate the CS-SGWFT matrix kernel. The CS-SGWFT holds the properties of the SGWFT including orthogonality, sequency ordered, approaching to the DFT and radix-2 fast algorithm implementation. Moreover, its conjugate symmetric property as the CS-SCHT is useful to process the pure real input data. We will show how the CS-SGWFT can gradually change the transformed signal from CS-SCHT to DFT results.

The organization of this paper is as follows: In section 2, we review the CS-DOT generating process proposed in [5]. In section 3, we propose CS-SGWFT as the CS-DOT special case and show its properties and the relationship between the CS-SCHT, CS-SGWFT and the DFT. In section 4, we apply the CS-SGWFT to image noise removal and spectrum estimation and show their benefit. Finally, we make conclusions in section 5.

2. CONJUGATE SYMMETRIC DISCRETE ORTHOGONAL TRANSFORM (CS-DOT)

In this section, we review the conjugate symmetric discrete orthogonal transform (CS-DOT) matrix for $N = 2^k$ in [5]. Let the periodic function $W(t)$ defined over $0 \leq t < 1$ which has the following properties:

P1. $W(t+1) = W(t)$

P2. $W(t) = \exp(ia(t))$ where $a(t)$ is a real for all t

This work was supported by the National Science Council, R.O.C. under Contract 98-2221-E-002-077-MY3.

P3. $W(t+1/2) = -W(t)$

P4. $W(-t+1/2) = -W^*(t)$ where * is conjugate symbol

From the above definition, we can generate an N by N CS-DOT matrix \mathbf{H} using the following procedure:

Step 1. Generating basis matrix \mathbf{U} as

$$U(k, r) = W(2^r k/N) = W(2^{(r-l)} k) \quad (1)$$

$$\text{For } 0 \leq r < l \text{ and } 0 \leq k < N$$

Step 2. From (1), we get l basis in terms of column vectors of \mathbf{U} . Then we can generate full rank matrix \mathbf{H} as

$$H(k, m) = \prod_{r=0}^{l-1} U(k, r)^{m_r} \quad 0 \leq m, k < N \text{ and } 0 \leq r < l \quad (2)$$

$$m = \langle m_{l-1}, m_{l-2}, m_{l-3}, \dots, m_0 \rangle_2 \quad (3)$$

m_r is the binary representation of m . By the definition of $W(t)$, we can realize that the degree of freedom of $U(k, 0)$ is $N/4$. For example, let $N = 16$ and set $U_{16}(0, 0) = 1$, according to **P1** to **P4**, we can express $U_{16}(k, 0)$ as

$$U_{16}(k, 0) = [1 \ w_1 \ w_2 \ w_3 \ w_4 \ -w_3^* \ -w_2^* \ -w_1^* \ -1 \ -w_1 \ -w_2 \ -w_3 \ -w_4 \ w_3^* \ w_2^* \ w_1^*] \quad (4)$$

That is, we can only set four parameters w_1, w_2, w_3, w_4 . From **P2** the values of $W(t)$ are on unity circle for all t and meanwhile $a(t)$ can be arbitrary real function. By the generating process (1) and (2), the elements of \mathbf{H} are all on unity circle and their absolute values are all equal to unity.

In [5], the conjugate symmetric property of \mathbf{H} is proved and it shows that the CS-DOT can also have radix-2 fast algorithm as well. The example for 16 points CS-DOT is shown in Fig. 1. Meanwhile, the conjugate symmetric sequency order Hadamard transform (CS-SCHT) and the DFT are shown as special cases of the CS-DOT. Finally, it also shows that the CS-DOT is useful to spectrum estimation.

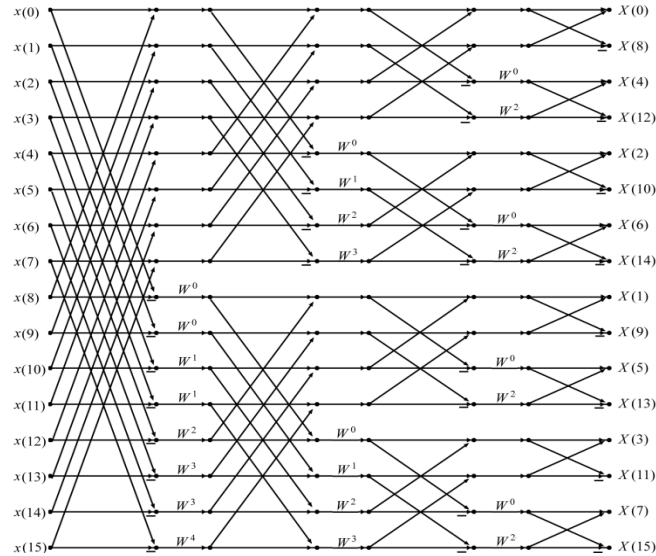


Fig. 1. CS-DOT signal flow diagram for $N = 16$

3. CS-SGWFT

We propose the conjugate symmetric sequency ordered generalized Walsh-Fourier Transform (CS-SGWFT) as the special case of the CS-DOT. We define conjugate symmetric generalized Rademacher function (CS-GRF) $\mathbf{R}_{p,cs}(t)$, which is modified version of the generalized Rademacher function (GRF) proposed in [6]. It has a simple controllable parameter p and is partially defined over four regions from $[0, 1/4)$, $[1/4, 1/2)$, $[1/2, 3/4)$ and $[3/4, 1)$ as

$$\mathbf{R}_{p,cs}(t)_{[0,1/4)} = \exp(-ik\pi/p) \quad t \in [k/p, (k+1)/p) \quad (5)$$

$$\mathbf{R}_{p,cs}(t)_{[1/4,1/2)} = -\mathbf{R}_{p,cs}^*(1/4-t)_{[0,1/4)} \quad (6)$$

$$\mathbf{R}_{p,cs}(t)_{[1/2,3/4)} = -\mathbf{R}_{p,cs}(t)_{[0,1/4)} \quad (7)$$

$$\mathbf{R}_{p,cs}(t)_{[3/4,1)} = \mathbf{R}_{p,cs}^*(1/4-t)_{[0,1/4)} \quad (8)$$

Where p is an integer and note that $\mathbf{R}_{p,cs}(t) = \mathbf{R}_{p,cs}(t+1)$.

From the above definition, we can use the one-quarter values defined in $[0, 1/4)$ to get the entire CS-GRF function according to the properties P3 and P4 of the $W(t)$ as follows:

$$W(t+1/2) = W^*(-t+1/2) = -W(t) \quad (9)$$

Let t' is shift by $1/4$ of t expressed as $t = 1/4 + t'$, from (5) to (8) we can get the following property symmetric to $t = 1/4$:

$$W(t+1/4) = -W^*(-t+1/4) \quad (10)$$

Therefore $W(t)$ is conjugate anti-symmetric to $t=1/2$ over $[0, 1/2)$ so that we can use one-quarter values to get entire values of $W(t)$. We can see that $\mathbf{R}_{p,cs}(t)$ satisfies the properties in P1 to P4. When we use $\mathbf{R}_{p,cs}(t)$ as the generating function to get the CS-DOT matrix, the obtained results is called the CS-SGWFT matrix. In addition to the CS-DOT properties such as conjugate symmetric, orthogonal, fast algorithm, the CS-SGWFT also has the following properties:

1. Generalization: When $p = 4$, the CS-SGWFT matrix $\mathbf{G}_{p,cs}$ is actually the conjugate of the CS-SCHT matrix in [3]. Here we will directly show that for $N = 16$, the CS-SGWFT matrix is

$$\mathbf{G}_{4,cs} = \begin{bmatrix} 1 & 1 & 1 & 1 & 1 & 1 & 1 & 1 & 1 & 1 & 1 & 1 & 1 & 1 & 1 & 1 \\ 1 & 1 & 1 & 1 & -j & -j & -j & -j & -1 & -1 & -1 & -1 & j & j & j & j \\ 1 & 1 & -j & -j & -1 & -1 & j & j & 1 & 1 & -j & -j & -1 & -1 & j & j \\ 1 & 1 & -1 & -1 & j & j & -j & -j & -1 & -1 & 1 & 1 & -j & -j & j & j \\ 1 & -j & -1 & j & 1 & -j & -1 & j & 1 & -j & -1 & j & 1 & -j & -1 & j \\ 1 & -1 & -1 & 1 & -j & j & j & -j & -1 & 1 & 1 & -1 & j & -j & -j & j \\ 1 & -1 & j & -j & -1 & 1 & -j & j & 1 & -1 & j & -j & -1 & 1 & -j & j \\ 1 & -1 & 1 & -1 & j & -j & j & -j & -1 & 1 & -1 & 1 & -j & j & -j & j \\ 1 & -1 & 1 & -1 & 1 & -1 & 1 & -1 & 1 & -1 & 1 & -1 & 1 & -1 & 1 & -1 \\ 1 & -1 & 1 & -1 & -j & j & -j & j & -1 & 1 & -1 & 1 & j & -j & j & -j \\ 1 & -1 & -j & j & -1 & 1 & j & -j & 1 & -1 & -j & j & -1 & 1 & j & -j \\ 1 & -1 & -1 & 1 & j & -j & -j & j & -1 & 1 & 1 & -1 & -j & j & -j & j \\ 1 & j & -1 & -j & 1 & j & -1 & -j & 1 & j & -1 & -j & 1 & j & -1 & -j \\ 1 & 1 & -1 & -1 & -j & -j & j & j & -1 & -1 & 1 & 1 & j & j & -j & -j \\ 1 & 1 & j & j & -1 & -1 & -j & -j & 1 & 1 & j & j & -1 & -1 & -j & -j \\ 1 & 1 & 1 & 1 & j & j & j & j & -1 & -1 & -1 & -1 & -j & -j & -j & -j \end{bmatrix} \quad (11)$$

Compared with the 16pts CS-SCHT matrix H_{16} generated by the method in [3], we can realize that the relationship between the CS-SGWFT matrix $\mathbf{G}_{4,cs}$ and H_{16} is

$$\mathbf{G}_{4,cs} = \mathbf{H}_{16}^* \quad (12)$$

We can see that although the CS-SGWFT for $p = 4$ and the CS-SCHT are the same, the generating process of the CS-SGWFT are much simpler and well structuralized than the CS-SCHT. Therefore, it is much easier for analyzing the properties and performances of the CS-SGWFT than the CS-SCHT.

On the other hand, when p grows larger, the CS-SGWFT approaches to the DFT in that the CS-GRF waveform defined in (5) to (8) is close to the sinusoidal function. That is, when p tends to infinity we can express $\mathbf{R}_{\infty,cs}(t)$ as:

$$\mathbf{R}_{\infty,cs}(t) = \exp(-i2\pi t) \quad (13)$$

$\mathbf{R}_{\infty,cs}(t)$ is exactly the sinusoidal function with frequency $f = 1$. Using the matrix generating process we can realize that the basis of $\mathbf{G}_{p,cs}$ is actually the same as the DFT matrix so that the CS-SGWFT is identical to the DFT. Especially, when p is a multiple of N ($p = aN$), we can express the values of $U(0,k)$ sampling from $\mathbf{R}_{p,cs}(t)$ as follows:

$$U(0,k) = \exp(-i2\pi k/N) \quad (14)$$

We can easily observe that $U(0,k)$ is exactly the first harmonic basis of the DFT matrix so that the CS-SGWFT and the DFT are exactly the same under $p = aN$ where a is an integer.

In Fig. 2 we plot the generalization relationships among the DOT, CS-DOT, CS-SGWFT, CS-SCHT and DFT and show the special case conditions.

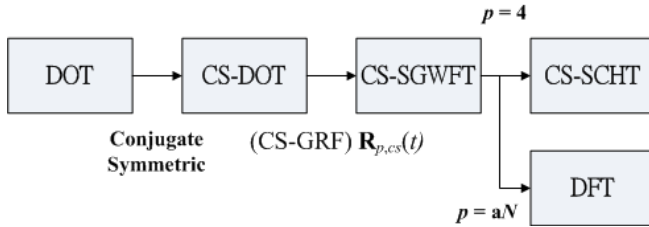


Fig. 2. Relationships among the CS-DOT, the CS-SGWFT, the CS-SCHT, and the DFT. The CS-SCHT and the DFT are the special cases of the CS-SGWFT where $p = 4$ and aN .

In Fig. 3, we can see that the CS-GRF waveforms gradually change from steps into the sinusoidal waveform. The number of steps gradually increases and the step size gradually decreases. For each CS-GRF $\mathbf{R}_{p,cs}(t)$, we can generate the orthogonal matrix $\mathbf{G}_{p,cs}$ using the CS-DOT generating process in the previous section. We call $\mathbf{G}_{p,cs}$ the conjugate symmetric sequency ordered generalized Walsh-Fourier transform (CS-SGWFT) matrix since the CS-SCHT and the DFT are the special cases of the CS-SGWFT where $p = 4$ and aN .

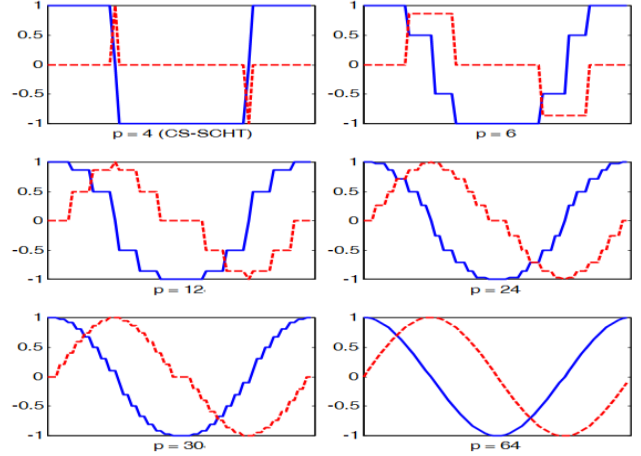


Fig. 3. Waveforms of the CS-GRFs for different phase quantization parameter p .

Let Δ denoted as the norm-2 (i.e., the maximum singular value) of the difference matrix between the CS-SGWFT matrix $\mathbf{G}_{p,cs}$ and the DFT matrix \mathbf{F} as follows:

$$\Delta = \left\| \mathbf{G}_{p,cs} - \mathbf{F} \right\|_2 \quad (15)$$

Let $N = 64$, we plot Δ versus p as the distance measurement in Fig. 4 and we can observe that the value of Δ decreases with p so that the CS-SGWFT approaches to the DFT when p grows larger.

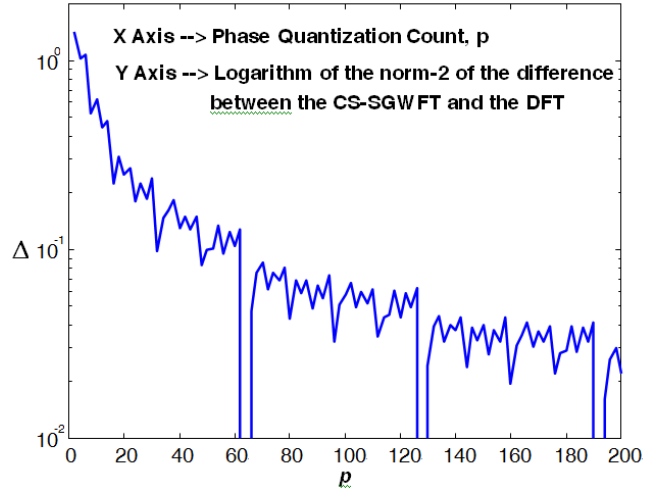


Fig. 4. The difference between the CS-SGWFT matrix and the DFT matrix for $N = 64$.

2. Sequency-Ordering: The CS-SGWFT basis arranges in the sequency order. Like the CS-SCHT, the zero crossing numbers in the m^{th} row of the CS-SGWFT matrix increases with m . For example, in Fig. 5, we plot the 2nd to the 9th rows of the CS-SGWFT matrix for $N = 64$ and $p = 10$. We realize that the number of zero crossings increases with m . Therefore, we can specify the low and high frequency com-

ponents of the signal so that the CS-SGWFT is suitable for spectrum analysis.

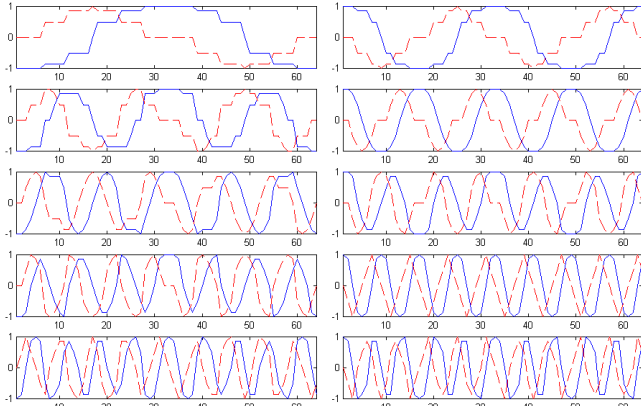


Fig. 5. The 2nd to the 9th rows in the CS-SGWFT matrix for $N = 64$ and $p = 10$. The solid and dash lines are the real and imaginary parts of the basis.

To show how the CS-SGWFT results change from the CS-SCHT to the DFT, we use the rectangular wave input signal as an example defined as

$$x(n) = \begin{cases} 1 & \text{for } n = 0 \text{ to } 4 \\ 0 & \text{for } n = 5 \text{ to } 64 \end{cases} \quad (16)$$

For $p = 2, 4, 8, 16, 32, 64$, the corresponding CS-SGWFT waveforms for each p are shown in Fig. 6. We can see that the transform results of the CS-SGWFT approach to that of the DFT when p increases.

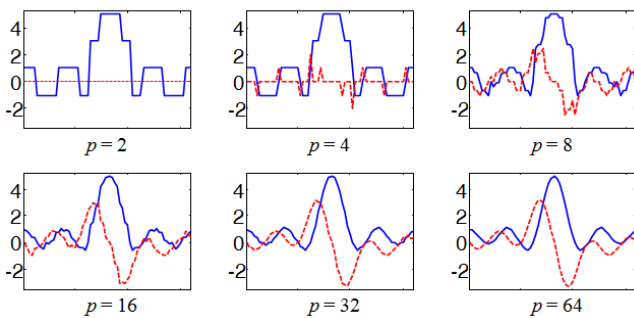


Fig. 6. Transform results of rectangular wave with different p in CS-SGWFT for $N = 64$ and $p = 2, 4, 8, 16, 32, \text{ and } 64$ from left to right and from top to bottom.

4. APPLICATIONS

4.1. Image Noise Removal

The CS-SGWFT is suitable for image interference removal under the circumstance that the interference is quantized sinusoidal signal so that the interference waveform looks like step-wise signals just as the CS-SGWFT basis. We show the block diagram of the image recovery process as in

Fig. 7. We can realize that for the inference signal $s(n)$ which can be modeled as linear spanned by quantized sinusoidal waveforms as follows

$$s(n) = \text{span} \left\{ \exp \left(\frac{-j2\pi k \lfloor n/m \rfloor m}{N} \right) \right\} \text{ for } k = 0, 1, 2, \dots \quad (17)$$

Using the SGWFT coding and low pass filtering we can have good performance in interference removal.



Fig. 7 Image interference removal block diagram

We use the contaminated ‘‘Lena’’ image recovery in Fig.8 as an example. From the example we can see that using CS-SGWFT for $p = 8$ has better signal recover performance than the other transforms. Therefore, we can realize that when the image is interfered by the quantization block signals, the CS-SGWFT can have better performance in recovery than the DFT.

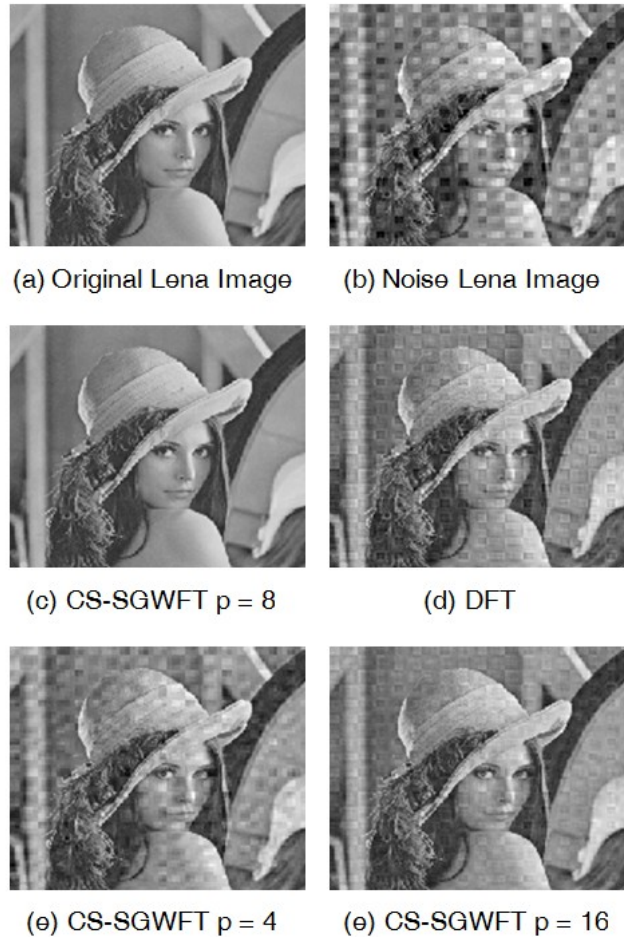


Fig. 8. Noise removal using CS-SGWFT. (a) original image (b) noised image (c) recovered image by CS-SGWFT for $p = 8$ (d)

recovered image by DFT (e) recovered image by CS-SGWFT for $p = 4$ (f) recovered image by CS-SGWFT for $p = 16$

4.2. Spectrum Estimation

In [3], it is shown that the CS-SCHT is suitable for spectral estimation in that the CS-SCHT has sequency order property as the DFT and we can specified the high and low sequency (frequency) region of the signal. For the CS-SGWFT, we can show that it is also suitable for spectrum estimation as the CS-SCHT and the DFT. We use the 3kHz sinusoidal waveform under sampling frequency 512kHz as an input example. We plot its 512 points DFT, CS-SCHT and CS-SGWFT ($p = 8$) magnitude spectrum in Fig. 9. Compared to the CS-SCHT, we can realize that the CS-SGWFT magnitude spectrum approaches more closely to the DFT spectrum. By the above example, we can see that the power compaction rate of the CS-SGWFT is about 85.7% ($(473.6/512)^2$) which is much higher than the CS-SCHT is (52.5%). Therefore it is better using the CS-SGWFT for $p = 8$ instead of the original CS-SCHT.

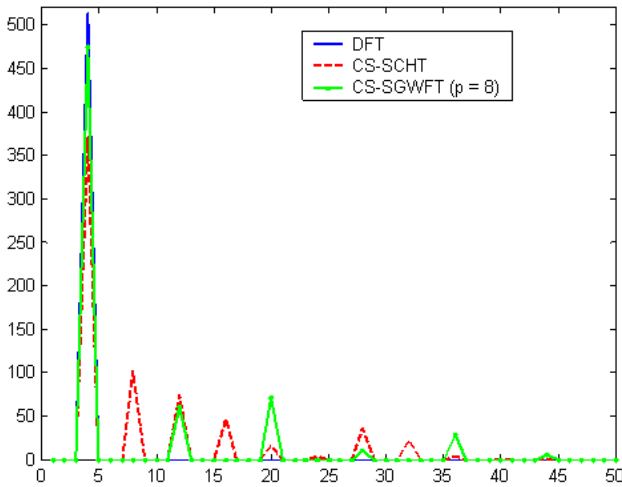


Fig. 9. Sinusoidal waveform magnitude spectrum of the CS-SCHT, CS-SGWFT ($p = 8$) and DFT

5. CONCLUSION

Based on the CS-DOT generating method, the CS-SGWFT, which generalizes the currently existing transforms, such as the CS-SCHT and the DFT, was proposed. As the original existing transforms, the proposed CS-SGWFT also has the conjugate symmetric, orthogonality and sequency ordering properties. Meanwhile, the CS-SGWFT also has the radix-2 fast implementation algorithms as the DFT does. In addition, we can easily switch the transform behavior from the CS-SCHT to DFT and we can observe that the result waveform morphing smoothly. Finally, we use signal noise removal as the applications of the CS-SGWFT. We believe that there will be more useful applications of the CS-SGWFT in the future.

REFERENCES

- [1] S. Rahardja and B. J. Falkowski, "Family of unified complex Hadamard transforms," *IEEE Trans. Circuits Syst. II, Analog Digit. Signal Process.*, vol. 46, no. 8, pp. 1094-1100, Aug. 1999.
- [2] A. Aung, B. P. Ng, and S. Rahardja, "Sequency-ordered complex Hadamard transform: Properties, computational complexity and applications," *IEEE Trans. Signal Processing*, vol. 56, no. 8, pp. 3562-3571, Aug. 2008.
- [3] A. Aung, B. P. Ng, and S. Rahardja, "Conjugate symmetric sequency ordered complex Hadamard transform," *IEEE Trans. Signal Process.*, vol. 57, pp. 2582-2593, Jul. 2009.
- [4] S.C. Pei, C.C. Wen, and J.J. Ding, "Sequency-ordered generalized Walsh-Fourier transform", *Signal Processing*, vol. 93, Issue 4, pp. 828-841, Apr. 2013.
- [5] S.C. Pei, C.C. Wen, and J.J. Ding, "Conjugate Symmetric Discrete Orthogonal Transform", *Circuits and Systems II: Express Briefs, IEEE Transactions on*, Accepted.
- [6] R. M. Aron, M. Lacruz, R. Ryan, and A. Tonge, "The generalized Rademacher functions," *Note di Matematica*, vol. 12, pp. 15-25, 1992.